NeuroImage 158 (2017) 176–185

Contents lists available at ScienceDirect

NeuroImage

journal homepage: www.elsevier.com/locate/neuroimage

Interoceptive signals impact visual processing: Cardiac modulation of visual body perception

Roberta Ronchi [a,b,*,1], Fosco Bernasconi [a,b,1], Christian Pfeiffer [a,b,c], Javier Bello-Ruiz [a,b], Mariia Kaliuzhna [a,b], Olaf Blanke [a,b,d]

[a] Laboratory of Cognitive Neuroscience, Brain Mind Institute, School of Life Sciences, Ecole Polytechnique Fédérale de Lausanne, Campus Biotech H4, Chemin des Mines 9, Geneva, Switzerland
[b] Center for Neuroprosthetics, School of Life Sciences, Ecole Polytechnique Fédérale de Lausanne, Lausanne, Switzerland
[c] Laboratoire de Recherche en Neuroimagerie, Department of Clinical Neurosciences, Lausanne University and University Hospital, Lausanne, Switzerland
[d] Neurology Division, Department of Clinical Neurosciences, Geneva University Hospital, Geneva, Switzerland

ARTICLE INFO

Keywords:
Body processing
Interoception
Cardio-visual stimulation
Visual-evoked potentials
Temporo-parietal cortex

ABSTRACT

Multisensory perception research has largely focused on exteroceptive signals, but recent evidence has revealed the integration of interoceptive signals with exteroceptive information. Such research revealed that heartbeat signals affect sensory (e.g., visual) processing: however, it is unknown how they impact the perception of body images. Here we linked our participants' heartbeat to visual stimuli and investigated the spatio-temporal brain dynamics of cardio-visual stimulation on the processing of human body images. We recorded visual evoked potentials with 64-channel electroencephalography while showing a body or a scrambled-body (control) that appeared at the frequency of the on-line recorded participants' heartbeat or not (not-synchronous, control). Extending earlier studies, we found a body-independent effect, with cardiac signals enhancing visual processing during two time periods (77–130 ms and 145–246 ms). Within the second (later) time-window we detected a second effect characterised by enhanced activity in parietal, temporo-occipital, inferior frontal, and right basal ganglia-insula regions, but only when non-scrambled body images were flashed synchronously with the heartbeat (208–224 ms). In conclusion, our results highlight the role of interoceptive information for the visual processing of human body pictures within a network integrating cardio-visual signals of relevance for perceptual and cognitive aspects of visual body processing.

1. Introduction

We live in a complex environment, receiving continuous multisensory information. Incoming signals are not limited to the external world (exteroceptive signals such as visual, auditory, or tactile signals), but also include information from the inside of our body (i.e. interoceptive signals) such as cardiac, respiratory and other visceral inputs. Up to now, data on how interoceptive and exteroceptive signals are integrated into the brain are still sparse. Previous neuroimaging research on multisensory integration has mainly focused on exteroceptive signals and extensively investigated how one sensory stimulus (e.g., a sound) influences the processing of another one (e.g., visual) (Stein and Stanford, 2008; van Atteveldt et al., 2014 for reviews). Studies in nonhuman primates described multisensory neurones in the inferior parietal sulcus responsive to combinations of visual, auditory and tactile stimuli (Andersen et al., 1997; Cohen and Andersen, 2004; Mazzoni et al., 1996; Schlack et al., 2005). Imaging studies in humans described multisensory responses in ventral premotor area and in parietal cortex, including inferior parietal and superior parietal lobules, as well as in primary cortices (such as primary visual cortex, Heschl's and superior temporal gyri) (Bushara et al., 1999; Calvert et al., 2000; Lewis and Van Essen, 2000; Bremmer et al., 2001; Calvert, 2001; Macaluso and Driver, 2001; Foxe et al., 2002; Pekkola et al., 2006; Martuzzi et al., 2007; Gentile et al., 2011). The importance of these brain regions for multisensory processing was extended by electrical neuroimaging studies, which investigated the spatio-temporal brain dynamics of visual-auditory, visual-tactile and audio-tactile integration. In favour of multisensory integration occurring within primary cortices, electroencephalography (EEG) studies found

* Corresponding author. Laboratory of Cognitive Neuroscience, Center for Neuroprosthetics, Ecole Polytechnique Fédérale de Lausanne (EPFL), Campus Biotech H4, Chemin des Mines 9, 1202, Geneva, Switzerland.
E-mail address: roberta.ronchi@epfl.ch (R. Ronchi).
[1] Co-first authors.

http://dx.doi.org/10.1016/j.neuroimage.2017.06.064
Received 3 January 2017; Received in revised form 19 June 2017; Accepted 22 June 2017
Available online 29 June 2017

early integration effects starting at 60 ms after stimulus onset, and during a later time-window (180 ms) (e.g., Molholm et al., 2002, 2006; Schürmann et al., 2002; Teder-Sälejärvi et al., 2002; Foxe and Schroeder, 2005; Cappe et al., 2010; Quinn et al., 2014). Early and late responses to multisensory stimulation in these regions were further supported by intracranial recordings in humans (Molholm et al., 2006).

Compared to these findings, there is currently only limited evidence about multisensory perception and integration of exteroceptive and interoceptive signals. For example, visual evoked potentials in response to basic visual stimuli (i.e., flashes) are enhanced when the visual stimulus is presented time-locked to the heartbeat (i.e., at the diastole) (Walker and Sandman, 1982). Moreover, recent studies demonstrated that the amplitude of the heartbeat-evoked potential (i.e., the cortical marker of cardiac processing) (Schandry and Montoya, 1996) is associated with changes in visual perception (Park et al., 2014; see also Park et al., 2016), and that conscious access for visual stimuli depends on when the stimulus is presented with respect to the participants' heartbeat (Salomon et al., 2016). Other research found that cardiac information facilitated the detection of emotional stimuli, such as fearful faces (Garfinkel et al., 2014). Related findings were reported in the auditory domain: presenting sounds in synchrony with the heartbeat resulted in a modulation of the auditory evoked potentials (van Elk et al., 2014). Even if it has been shown that cardiac signals modulate the processing of visual stimuli, it is currently unknown if and how interoception influences the visual perception of human bodies.

The processing of visual images of the human body has been linked to a dedicated network consisting of the extrastriate body area and the fusiform body area in the temporo-occipital cortex. These two regions respond strongest to the appearance of human bodies or human body parts compared to other stimuli such as houses (Downing et al., 2001; Peelen and Downing, 2007; Downing and Peelen, 2011), and process bodily features as shape and posture (Downing and Peelen, 2016). In addition to functional magnetic resonance imaging (fMRI) studies, important data about temporal and spectral aspects of the body-specific processing in the extrastriate cortex has been provided by magnetencephalography and EEG studies. Thus, a first activation occurs during the categorization of the bodily image (at 100 ms: P1) (de Gelder et al., 2010), followed by activations that are associated with a more refined structural body-specific processing, occurring between 150 and 250 ms after stimulus onset (N190) (Thierry et al., 2006; Ishizu et al., 2010). These activations are found within the temporo-occipital cortex, likely overlapping with the extrastriate body area (see Barraclough et al., 2006; Pourtois et al., 2007). Although several studies have supported the role of the extrastriate body area in multisensory (e.g., visuo-auditory) integration (Beer et al., 2013; Limanowski and Blankenburg, 2016), it is debated if this area is a unimodal visual area or an important region for multisensory bodily processing (Downing and Peelen, 2011). Moreover, to date no EEG study has reported interoceptive modulation during the visual processing of human bodies, and such processing has recently been linked to self-related brain processes (Blanke, 2014). Thus, behavioural data showed that seeing a body/body-part image flashing at the same frequency of the subject's heartbeat (i.e., cardio-visual stimulation) induces an alteration in the sense of body ownership and self-location. This was found in healthy subjects (Aspell et al., 2013; Suzuki et al., 2013) and a neurological patient (Ronchi et al., 2015).

Extending these findings, we asked whether brain activity related to the processing of the human body can be modulated by interoceptive information. This is a topic of particular relevance for at least two reasons: i) our sense of self, and the link between bodily processing and the sense of self, is based on the integration of exteroceptive and interoceptive bodily signals (Craig, 2002; Blanke, 2012), and ii) only little is known about the neural mechanisms of this integration. Here, we investigated whether an interoceptive signal, the heartbeat, modulates brain activity related to the visual processing of a human body and sought to determine the electrophysiological brain mechanisms of such cardio-visual processing. We recorded 64-channel EEG and analysed visual evoked potentials (VEPs) during the presentation of visual body images synchronised (or not) with participants' own online detected heartbeat. According to previous evidence, we predicted that cardio-visual synchrony would affect VEPs in response to human bodies. The specificity of cardio-visual effects on the visual processing of bodily stimuli was tested by repeating the same conditions for scrambled bodies.

2. Materials and methods

2.1. Participants

Sixteen healthy right-handed participants (2 females, mean age: 26.8 ± 2.8, range: 23–31) took part in this experiment, approved by the Ethical Committee of the Brain and Mind Institute at EPFL, Lausanne. Two participants were excluded due to excessive muscle artefacts contaminating the EEG signal, leaving 14 participants for the analyses. All participants gave their written informed consent prior to study participation.

2.2. Procedure

Participants were seated in a dark and sound attenuated room at a distance of 60 cm from an LCD screen (27-inch monitor, refresh rate of 120 Hz). Participants' electrocardiogram (ECG) was recorded for the entire session. ECG data were acquired by an Arduino™ microcontroller with a mounted e-Health Sensor Shield V2.0 from Libelium™ through three electrodes placed on the chest (two at the level of the left and right clavicles, the third one on the left side at the last rib). The in-house software detected, in real time, the R peak of the QRS complex (amplitude change over 80% of the difference between the exponential moving averages of the maxima and minima of the raw signal).

The experiment was composed of a total of 22 blocks. At the beginning of each block, the monitor displayed a black background and a red fixation point (visual angle: 0.3°) positioned in the centre of the screen. Participants were instructed to fixate the red dot throughout the whole block. The visual body stimuli were presented centrally on which a red fixation dot was presented, such that the fixation dot was always in the same location on the screen. The visual stimuli were of two categories: 1) Body-intact: a picture of a body from behind; and 2) Body-scrambled: the same picture of a body from behind but in a scrambled version, i.e. with the body divided into 5 parts (see Soria Bauser and Suchan, 2013). In the scrambled version, body parts were maintained in the original upright position (see Fig. 1). Both intact and scrambled body images were presented on the screen in one of the two following categories with respect to the heartbeat: 1) Synchronous (S): the body appeared synchronously with respect to the QRS complex (with a constant delay of 40 ms after detection of the R peak); 2) Non-Synchronous (NS): the body appeared randomly and out of phase with respect to the QRS complex of the participant. The stimulus was presented at a time interval of 900 ± 200 ms, accordingly to the control condition of a previous study about cardio-auditory integration (van Elk et al., 2014). We performed a two by two factorial design, with Factor 1: Stimulus (i.e. intact or scrambled), and Factor 2: Heart (i.e., S or NS), for a total of four experimental conditions. Each block of the four conditions lasted one minute and was repeated five times, for a total of 20 experimental blocks. The order of the 20 blocks was randomised across participants. Every stimulus presentation lasted 249 ms. The visual image subtended a maximum of 12° of visual angle. In addition to the above-described 20 blocks, two resting blocks (duration: 2.5 min each) were performed before and after the experiment (total duration: 5 min, as each experimental condition). During the resting block, no visual stimuli were presented (except for the red fixation dot); the participants' EEG was recorded while they were asked to look at the black monitor. The inclusion of the resting blocks was necessary to remove the cardiac artefact present in the EEG signal (Montoya et al., 1993; van Elk et al., 2014). Fig. 2 shows the schematic diagram of the experiment.

Fig. 1. The image of the two stimuli presented during the experiment: the Body-intact (on the left-side) and the Body-scrambled (on the right-side).

2.3. Electroencephalography recording and pre-processing

EEG was recorded continuously at 2048 Hz sampling rate using a Biosemi Active-Two System (BioSemi, Amsterdam, Netherlands) from 64 active scalp electrodes according to the standard 10/20 system. The recording was referenced to the "common mode sense" (CMS; active electrode) and grounded to the "driven right leg" (DRL; passive electrode), which functions as a feedback loop driving the average potential across the electrode montage to the amplifier zero. EEG epochs were time-locked to the onset of the visual stimuli. To verify the exact time of visual stimulus appearance, we recorded the stimulus onset with a photodiode situated on the monitor. Pre-processing and data analyses were done using Cartool (Brunet et al., 2011) and customised MATLAB scripts. Data were down-sampled to 1024 Hz. Signals were filtered with a band-pass filter of 1–40 Hz. Artefacts were removed by: i) visual inspection of the data; we rejected trials if several channels showed non-stereotypical artefacts that did not repeat on other trials based. If only a single channel showed a non-stereotypical artefact, this channel was interpolated for that trial only using a custom-written function. ii) Independent component analysis (ICA) was applied to the remaining trials. ICA components reflecting eye blinks or noise were identified and removed using a custom-written plugin (Chaumon et al., 2015). iii) Electrodes with noisy signal across a large range of epochs were replaced by interpolating neighbouring channels after the ICA procedure (Perrin et al., 1987). Finally, all epochs were inspected again for remaining noise or blinks not removed by the ICA and rejected if artefacts had remained.

In order to remove the cardiac artefact from the EEG signal, we averaged the EEG epochs of the resting condition, in which no visual stimulation was delivered and the epochs were time-locked with the R-peak, and we subtracted the mean heart resting condition signal to each heartbeat epoch present in the four conditions of interest (Body-Intact S, Body-Scrambled S, Body-Intact NS, Body-Scrambled NS).

As we were interested in analysing the earlier components of the VEPs in response to the body images (i.e., the P100 and N170), EEG epochs were defined from 100 ms pre-stimulus to 300 ms post-stimulus onset: the epochs were averaged for each participant to calculate visual evoked potentials (VEPs) for each condition. Baseline correction on the 100 ms pre-stimulus onset was applied. The average numbers (±SEM) of accepted EEG epochs for each condition were: Body-Intact S = 341.25 ± 10.6; Body-Scrambled S = 337.06 ± 10.8; Body-Intact NS = 322.05 ± 2.18; Body-Scrambled NS = 315.5 ± 5.65. The number of accepted epochs did not differ significantly across conditions (ANOVA Stimulus by Heart. Main effect of Heart: $F = 3.05$; $p > 0.1$; Main effect of Stimulus: $F = 1.77$; $p > 0.2$; Interaction Stimulus by Heart: $F = 1.77$; $p > 0.2$): therefore, we can exclude that the effects found depended on differences in signal-to-noise ratios.

2.4. EEG analyses and source estimation

2.4.1. General analysis procedure

Here we applied the stepwise analysis procedure referred as electrical neuroimaging. First, we applied a canonical VEPs analysis, to facilitate the comparison of our results with previous literature. As a second step in our analysis, we computed reference-independent measures such as Global Field Power (GFP) and topographical analysis, providing us with full data-driven results, free of any a priori assumptions.

2.4.2. Voltage waveform analyses

As a first level of analysis, the VEPs data were analysed with a repeated measure non-parametric ANOVA (re-estimated via 1000 bootstrap resamples) with Stimulus (two levels: Intact – Scrambled) and Heart (two levels: S – NS) as within-subject factors, performed on one exemplary scalp electrode (PO7) as a function of peri-stimulus time. Only effects exceeding the p-value< 0.05 criterion, for at ~15 consecutive milliseconds (15 continuous data points), were considered reliable (Guthrie and Buchwald, 1991; Bernasconi et al., 2014). This analysis was included to give an impression of specific effects within the dataset, and to facilitate the contextualisation of our results with respect to other VEP studies on body processing (e.g., Thierry et al., 2006; Soria Bauser and Suchan, 2013). However, due to the electrode reference-dependent

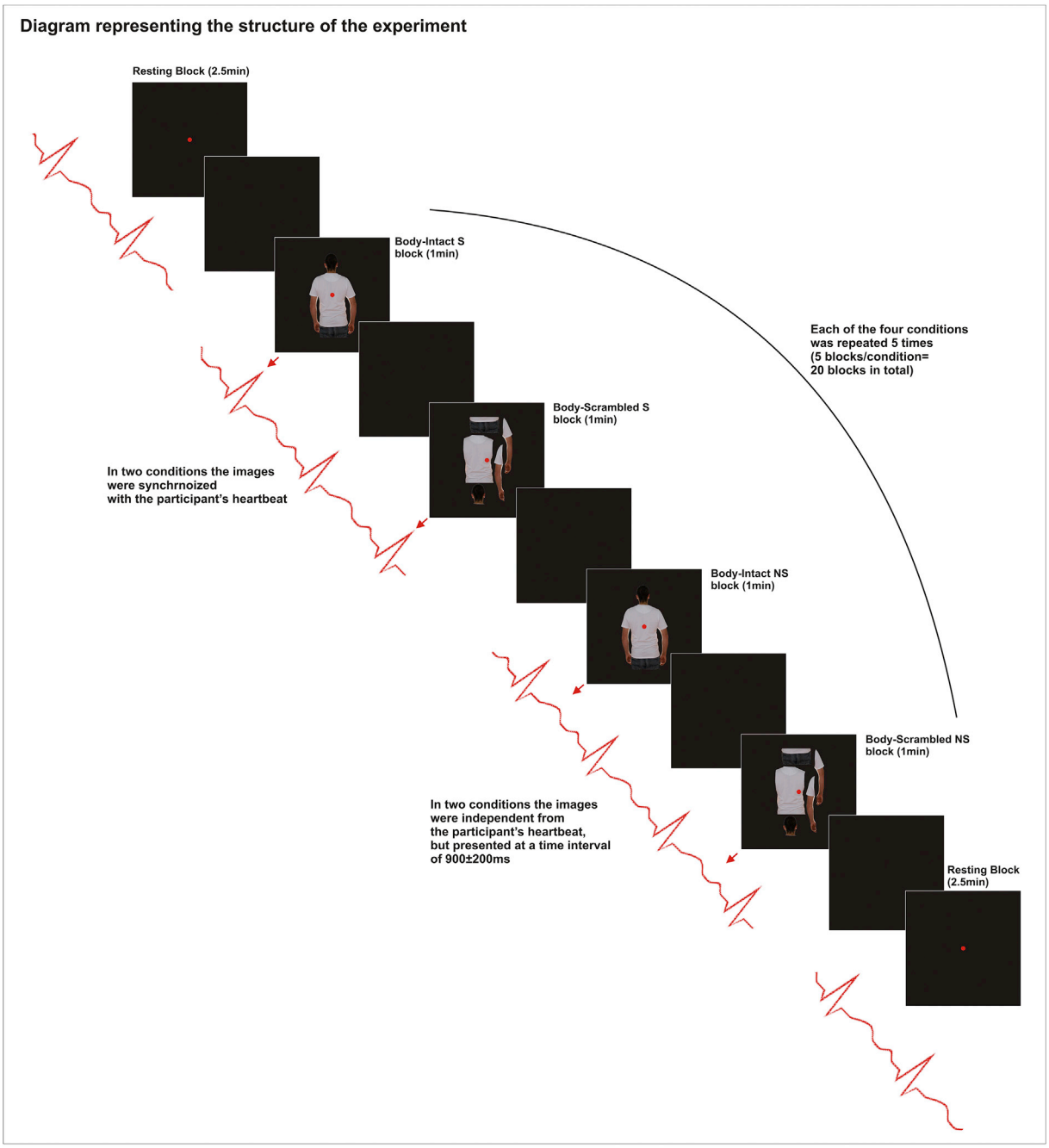

Fig. 2. Schematic representation of the experimental procedure. Every participant started and finished the experiment with a resting block (2.5min for each block), in which no visual stimulation was provided but the heartbeat of the participant was recorded. Following the first resting block, the four conditions (Body-Intact S, Body-Scrambled S, Body-Intact NS, Body-Scrambled NS) were administered in blocks of 1 min (i.e., 5 blocks of 1 min for each condition), in a random order. During the S conditions, the appearance of the image was synchronised with the R-peak of each participant, recorded on-line; during the NS conditions, the appearance of the image was not linked to the heartbeat of the participant. Each stimulus's duration was of 249 ms.

nature of these statistical analyses, our primary analyses and basis for interpretation were the electrode reference-independent analyses detailed below.

2.4.3. *Topographic modulation analyses*

In order to test the VEPs topography independent of its strength, we used a Global Map Dissimilarity (GMD) (Lehmann and Skrandies, 1980), which is calculated as the root mean square of the difference between 2 strength-normalized vectors (i.e., the instantaneous voltage potentials across the electrode montage). The GMD values between the body's images processing as a function of the heart feedback were compared time-point by time-point with an empirical distribution derived from a bootstrapping procedure (1000 permutations per data point), based on randomly reassigning data across conditions for each participants (detailed in Murray et al., 2008; Koenig et al., 2011). GMD is an electrode reference-independent analysis. Moreover, GFP and GMD are two orthogonal analyses because GMD is insensitive to pure amplitude modulations across conditions (see paragraph 2.4.4). A topographic modulation is neurophysiologically interpreted as a change in the configuration of the underlying active sources (Lehmann, 1987). A temporal autocorrelation was corrected through the application of a ~15 continuous milliseconds (15 continuous data points) threshold, as a

temporal criterion for the persistence of significant effects.

2.4.4. Global electric field analyses

Changes in the global electric field strength were calculated using the GFP, a reference electrode-independent analysis (Murray et al., 2008; Koenig and Melie-García, 2010), for each participant and experimental condition. The GFP measures the strength of the electric field at the scalp, and is equivalent to the standard deviation of the voltage potential values across the entire electrode montage at a given time point (Murray et al., 2008). Modulations in GFP were statistically analysed over the periods of interest defined by the above topographic cluster analysis (similar approach in multisensory studies, e.g., Cappe et al., 2012). A non-parametric ANOVA (re-estimated via 1000 bootstrap resamples) with Stimulus (two levels: Intact – Scrambled) and Heart (two levels: S – NS) as within-subject factors was performed at each scalp electrode as a function of peri-stimulus time. Only effects exceeding the p-value< 0.05 criterion, for at ~15 consecutive milliseconds (15 continuous data points), were considered reliable (Guthrie and Buchwald, 1991; Bernasconi et al., 2014).

2.4.5. Source estimations

We estimated the localisation of the electrical activity in the brain using a distributed linear inverse solution applying the local autoregressive average regularisation approach (LAURA), comprising biophysical laws as constraints (Grave de Peralta Menendez et al., 2001, 2004; Michel et al., 2004). For the lead field matrix calculation, we applied the spherical model with anatomical constraints (SMAC) method (Spinelli et al., 2000), which transforms the MRI to the best-fitting sphere using homogeneous transformation operators. The solution space included 3005 nodes in the grey matter of this spherical MRI and computed the lead field matrix using the known analytical solution for a spherical head model with 3 shells of different conductivities as defined by Ary et al. (1981). The time periods indicating significant GMD and/or GFP modulations across conditions were used as the periods of interest on which to carry out the source estimations. To increase the signal-to-noise ratio, VEPs for each participant and each experimental condition were separately averaged across the time periods indicating significant modulation in GMD and/or GFP. To assess the intracranial sources generating the interaction, the inverse solution was then estimated for each of the 3005 nodes. These data were then submitted to a two-way ANOVA using Stimulus and Heart as within-subject factors. To correct for multiple testing, only nodes with p-values <0.05 two-tailed and clusters of at least 17 contiguous significant nodes were considered reliable (this criterion was published elsewhere, e.g., Thelen et al., 2012). This spatial criterion was determined using the AlphaSim program (available at http://afni.nimh.nih.gov) and assuming a spatial smoothing of 6 mm full-width half maximum. This criterion indicates that there is a 3.54% probability of a cluster of at least 17 contiguous nodes, which gives an equivalent node-level p-value of $p \leq 0.0002$. The results of source estimations were rendered on the Montreal Neurological Institute's average brain with the Talairach and Tournoux (1988) coordinates.

3. Results

3.1. VEPs waveform analyses

The first level of VEP analysis to body-stimuli across conditions was based on the visual inspection of a selected posterior electrode (i.e., PO7), which has previously been found to be associated with the processing of visual bodies and scrambled bodies (van Heijnsbergen et al., 2007; Soria Bauser and Suchan, 2013). Statistical VEP analysis at PO7 with a two by two (Stimulus by Heart) factorial ANOVA (as a function of peri-stimulus time and for each time-point) revealed a significant interaction between Stimulus and Heart (p< 0.05, >15 consecutive milliseconds) for the time period from 190 to 228 ms post-stimulus onset (see Fig. 3A–B). Moreover, a significant main effect of Heart was found during three periods (88–130 ms, 148–174 ms and 194–238 ms post-stimulus onset) and a significant main effect of the Stimulus was found from 142 to 177 ms post-stimulus onset.

3.2. Topographic modulation and global field power analyses

The time-point by time-point ANOVA on GMD (p-value< 0.05, >15 consecutive milliseconds) resulted in a significant main effect of Stimulus in the time periods 110–186 ms and 213–274 ms post-stimulus onset, and a significant main effect of Heart during the time periods 77–130 ms and 145–246 ms post-stimulus onset. These effects imply the presence of different configurations of the underlying brain activity for the visual body and for cardio-visual synchrony. No interaction Stimulus by Heart was observed for GMD.

We next analysed changes in global electric field strength: for this, we used the significant time periods with the main effect of Heart or Stimulus using GMD analyses. This approach was chosen for two main reasons: first, we wanted to assess if the change in source configuration were also characterised by a change in amplitude of the response; second, defining a period of interest reduces the multiple comparisons. We computed the mean GFP for each condition and for each subject. Statistical analysis (two-way ANOVA) on the main factor Heart revealed for both time periods of interest (77–130 ms and 145–246 ms) a stronger amplitude for stimuli presented in synchrony with the heartbeat (first time period: $F_{1,13} = 59.7$; $p < 0.001$; second time period: $F_{1,13} = 5.40$; $p = 0.037$). We also found that the latency of the GFP peak within the first time period occurred significantly earlier for S stimuli as compared to NS stimuli (mean latency ± SEM: Body-Intact S = 123±3 ms; Body-Scrambled S = 224±2 ms; Body-Intact NS = 232±2 ms; Body-Scrambled NS = 231±2 ms) ($F_{1,13} = 13.74$; $p < 0.01$). With respect to the main effect of Stimulus for each condition and for each subject, statistical analyses on the mean GFP calculated for the two time periods suggested by GMD (110–186 ms and 213–274 ms) revealed only for the second time period an enhanced response for intact vs. scrambled bodies ($F_{1,13} = 14.67$; $p = 0.002$) (first time period: $F_{1,13} = 1.17$; $p = 0.299$).

We next assessed whether there was a synchrony-dependent effect of cardiac stimulation on visual body processing (i.e., Stimulus by Heart interaction) by analysing the GFP over the two time periods showing a main effect of Heart (i.e., 77–130 ms and 145–246 ms post-stimulus onset). This analysis revealed a significant Stimulus by Heart interaction over the period 208–224 ms ($F_{1,13} = 14.82$; $p = 0.002$) (see Fig. 3C-D-E). Post-hoc multiple comparisons were performed over the average of the above-mentioned period showing a significant interaction (i.e., 208–224 ms), and a Bonferroni correction was applied to correct for multiple comparisons by dividing the alpha level (i.e., 0.05) by the number of comparisons performed (i.e., N = 6), with a significant p-value set at $p < 0.008$. The results demonstrated a significant increase in GFP for the vision of a Body-Intact vs. Body-Scrambled only when presented synchronously with the heartbeat ($p < 0.001$ Bonferroni corrected), while the difference between Body-Intact and Body-Scrambled was not significant for the NS condition (Fig. 3 F). We note that we obtained similar results when the analyses were run without the subtraction of the cardiac artefact (see Material and Method section).

3.3. Source estimations

Brain activity associated with the Stimulus by Heart interaction (208–224 ms post-stimulus period, averaged; $F_{1,13} > 4.5$; p-values< 0.05; ke > 17 contiguous solution points) included the left parietal cortex (including post-central gyrus, inferior parietal lobule, and angular gyrus), left temporo-occipital areas (including the superior temporal gyrus, middle temporal gyrus and middle occipital area), the right frontal lobe (inferior gyrus), the right basal ganglia extending into the right insula and the right anterior cingulate cortex (the maximum was localized on the left superior temporal gyrus, Talairach coordinates: −61, −48, 10)

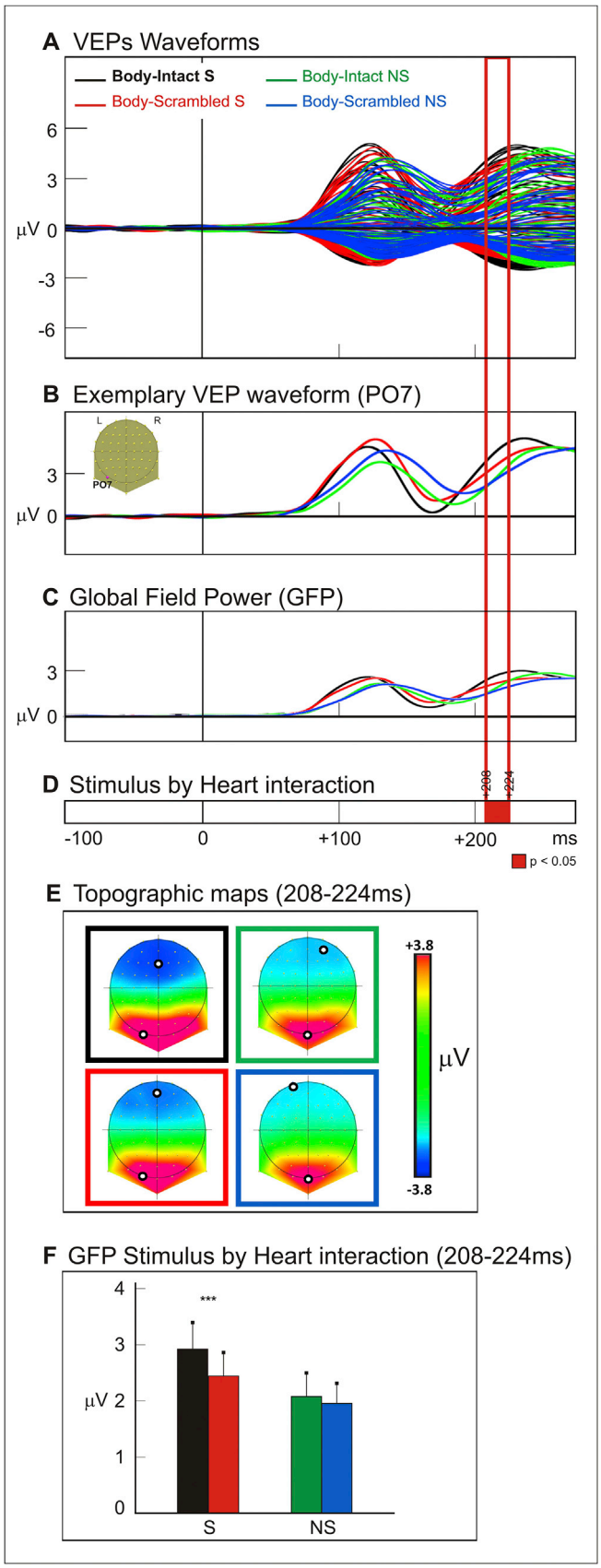

Fig. 3. Electrical neuroimaging results. A) The VEPs waveforms (64 electrodes) in response to the Body-Intact (black) and Body-Scrambled (red) images time-locked to the R-peak, and in response to the Body-Intact (green) and Body-Scrambled (blue) images not time-locked to the R-peak, are shown. B) VEPs on one exemplary left occipito-parietal electrode (PO7). C) Global Field Power (GFP) in response to each condition is shown. D) A two-way ANOVA was performed time-point by time-point, over the whole epoch length. The red box indicates the period of significant Stimulus by Heart interaction (p-values < 0.05), 208–224 ms after the stimulus onset. E) Topographies for each experimental condition: Body-Intact (black box) and Body-Scrambled (red box) time-locked to the R-peak, and Body-Intact (green box) and Body-Scrambled (blue box) not time-locked to the R-peak, are shown for the time period of significant interaction. F) The GFP effect is quantified over the average period 208–224 ms: the difference between Body-Intact and Body-Scrambled is significant only for synchronous stimulation.

(see Fig. 4). Brain activity associated with the main effect of Heart was calculated separately for the 77–130 ms and for the 145–246 ms post-stimulus periods. For the first time period, source estimation analysis showed the strongest activation in the left superior temporal gyrus (Talairach coordinates: −64, −27, 9) and for the second time period in the left superior frontal gyrus (Talairach coordinates: −31, 18, 52). The same analysis for the main effect of Stimulus (periods 110–186 ms and 213–274 ms) revealed for the first period strongest activity in the left frontal pre-central gyrus (Talairach coordinates: −53, −36, 36) and for the second time period on the right frontal pre-central gyrus (Talairach coordinates: 33, −27, 57).

4. Discussion

In the present study, we have investigated the impact of interoceptive (i.e., cardiac) signals on visual processing, in particular the question whether interoceptive signals influence the neural processing of body images. Previous research using EEG and fMRI addressed a related topic showing that interoceptive stimuli can modulate (e.g., enhance or suppress) the processing of basic visual stimuli such as dots or flashes (Walker and Sandman, 1982; Park et al., 2014; Salomon et al., 2016). The brain regions mainly responsible for this modulation are the insula, the cingulate cortex, the ventromedial prefrontal region and the inferior parietal lobe. Other recent evidence using fMRI also demonstrated that cardiac inputs may facilitate the detection of emotional faces: this effect was associated with greater neural responses in the amygdala (Garfinkel et al., 2014). The present study targets the timing of cardiac modulatory effects on visual processing and extends these earlier data by revealing distinct periods of stimulus-locked brain activation that reflect the impact of heartbeat signals on the visual processing of human bodies.

We found a *synchronous cardio-visual effect* modulating VEPs during two time periods: an early effect starting at 77 ms and a later effect from 145 to 246 ms, both characterised by different topographies between synchronous and non-synchronous cardio-visual stimulation (independent of whether the body was shown as scrambled or not). Moreover, these brain activations were enhanced during synchronous stimulation during both time periods, peaking around the P100 component and during later components, the N170 and P2, of visual processing. These data show that cardiac signals impact brain activity during two prominent steps of visual information processing: an early period that has been linked to the first categorization of the image and a later component that is important for complex visual processing including faces and human bodies (Thierry et al., 2006; de Gelder et al., 2010). Only a few studies have investigated when the neural processing of sensory signals is modulated by internal visceral signals such as the heartbeat. With respect to visual processing, Walker and Sandman reported that a visual flash presented at the diastole (that is around the ECG R-peak, as in the current study) induces a larger amplitude of VEPs, especially of the P1 component (Walker and Sandman, 1982), compatible with the present results. In the field of pain processing, previous studies also reported differential activation strength with stimuli presented at the systole (around the ECG T-peak) vs. the diastole for pain-related potentials (Edwards et al., 2008; Gray et al., 2010). These findings have be contextualized within the baroreceptor model (Koriath and Lindholm, 1986), which assumes that sensory processing is globally enhanced if the stimulus is associated with the diastolic phase of the cardiac cycle (the R-peak) while the

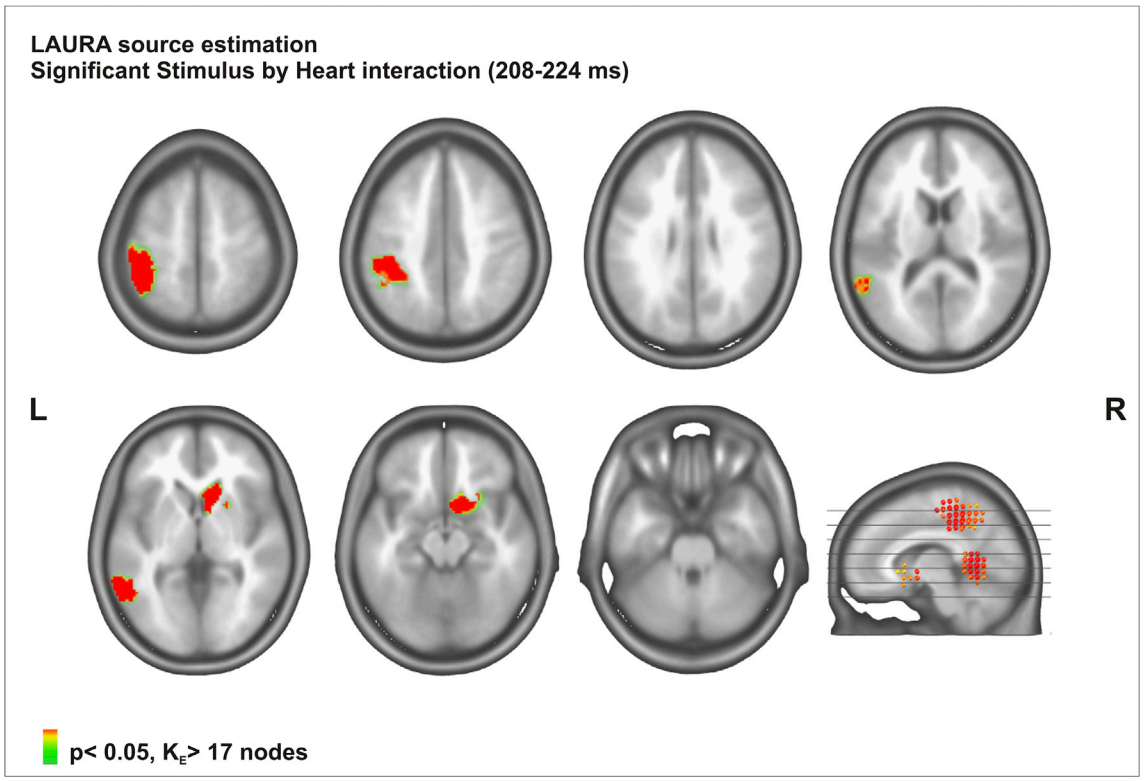

Fig. 4. Source Estimation. Statistical contrast (two-way ANOVA) across all solution points during the period of GFP modulation (208–224 ms post-stimulus onset) reveals a significant Stimulus by Heart interaction ($p < 0.05$) within the left parietal lobule, the left temporo-occipital regions, the right inferior frontal cortex, the right basal ganglia-insula and the right anterior cingulate.

baroreceptors were silent (compared to the systolic phase, the T-Peak, when the sensory processing is mainly inhibitory). Even if it has been shown that visual processing is not always inhibited at systole, at least in the domain of emotional stimuli processing (Garfinkel et al., 2014), the present data support the baroreceptor model of enhancement and allow refining it: in fact, we demonstrate that visual processing, when the stimulus is presented at the diastole, is not enhanced globally, but during two specific time periods following the stimulus onset (i.e., during the P1 and P2 components). Although not directly tested in the present study, we argue that such differential effects may reflect more general enhancement during the earlier P1 component and a later enhancement of more bodily processing effects during the N170/P2 period. Additionally, such stimulus-independent cardiac enhancements may also relate to the presence of multisensory effects between interoceptive (cardiac) and exteroceptive (visual) signals that are boosted in synchronous versus asynchronous stimulations (Aspell et al., 2013; Suzuki et al., 2013; Ronchi et al., 2015; Park et al., 2016). The latter hypothesis would be compatible and extend previous electrophysiological findings about the presence of early (Giard and Peronnet, 1999; Molholm et al., 2002; Cappe et al., 2010) and late (Giard and Peronnet, 1999; Fort et al., 2002; Molholm et al., 2002) modulation of VEP components by a second co-presented exteroceptive (e.g., auditory) stimulus. Further supporting this multisensory proposal, we note that the timing of the present cardio-visual effect is in line with those reported in audio-visual studies (Fort et al., 2002; Molholm et al., 2002; Cappe et al., 2010). Our second cardio-visual time period somewhat exceeds the second audio-visual integration effect, suggesting that the modulation of visual processing driven by interoceptive information may extend up to 250 ms after stimulus onset. However, more work is needed directly comparing bimodal exteroceptive effects with bimodal intero-exteroceptive ones. We argue that it is unlikely that these effects are due to an artefact directly produced by the heartbeat on VEPs or by a heartbeat evoked potential on the present VEPs because we removed the "cardiac component" (Montoya et al., 1993; van Elk et al., 2014) from the EEG data prior to calculating VEPs. Importantly, the subtraction of the cardiac artefact did not cause our results, as the direction of our findings is also present before the subtraction. To sum up, the synchronous cardio-visual effects is compatible with and extends past evidence (e.g., Walker and Sandman, 1982) about the modulation of visual processing during the diastole (i.e., the R-peak), and links such modulatory processing to two distinct time periods.

Importantly, our data reveal the presence of a distinct brain activation pattern that partly overlapped with the late cardio-visual enhancement effect, and was modulated by the vision of an intact human body stimulus. Whereas previous work had reported that interoceptive signals modulate the processing of basic visual stimuli and emotional faces, we here provide evidence for the enhancement of visual processing when a full body is shown as compared to a scrambled body, and only when in synchrony with the participants' heartbeat. The latency of this *synchronous cardio-visual effect on bodily processing* (i.e., from 208 to 224 ms after the stimulus onset) suggests that cardiac signals do not modulate the early categorization of the picture of a human body (i.e., the P1 component; see Thierry et al., 2006; Pourtois et al., 2007; de Gelder et al., 2010), but only the later more specialised visual body processing steps. These higher-level processes, likely reflected by visual and dorsal stream areas involved in the configurational elaboration of the human body, have been modulated by comparisons of whole bodies versus rotated or scrambled bodies (Soria Bauser and Suchan, 2013; Brandman and Yovel, 2016). Thus, the time-window of our *synchronous cardio-visual effect on bodily processing* shortly follows the peak of the N190 (Urgesi et al., 2004; Thierry et al., 2006; Peelen and Downing, 2007; Pourtois et al., 2007) and precedes the peak of the P2 component (Peelen and Downing, 2007). The N190 component has been related to visual coding of human bodies vs. other stimuli (Thierry et al., 2006), whereas the subsequent P2 component has been proposed to respond to the configurational processing of the body. In fact, the P2 amplitude is reduced by the distortion of bodies images, as for example by displacing a hand from a normal

position to a physically impossible position (Gliga and Dehaene-Lambertz, 2005), and enhanced when seeing body parts in a physically possible "gestalt" configuration (Vakli et al., 2016). Thus, our data show that an internal bodily signal, i.e. the heartbeat, shapes precise visual processing steps for complex aspects of the human body, during which we also found evidence for a more general, stimulus-independent, enhancement of visual processing as based on cardiac input (see the previous paragraph).

Which brain regions were activated during the present *synchronous cardio-visual effect on bodily processing*? Source estimations over this time period located this effect within parietal (inferior parietal areas including angular gyrus, post-central gyrus), temporo-occipital (superior temporal gyrus, middle temporal gyrus and middle occipital area) and inferior frontal cortex, as well as the basal ganglia and the insula. Fronto-insular-parietal networks have been linked to cardiac processing before (Critchley et al., 2004; Khalsa et al., 2009; Wiebking et al., 2014) and we found enhanced brain activity in these regions coding for interoceptive signals only when the image of the human body was presented in synchrony with the heartbeat (*synchronous cardio-visual effect on bodily processing*). Thus, the latter effect cannot only be explained by the cardiac processing, as it was only found for unscrambled body images. Frontal and parietal regions, particularly the posterior parietal cortex, are involved in the multisensory integration of inputs relevant to the body, as stimuli close and possibly interacting with our body parts (Serino et al., 2011; Brozzoli et al., 2012; Blanke et al., 2015). Moreover, parietal regions are strongly involved in the representation not only of the space surrounding the body but of the body itself (Daprati et al., 2010; Tsakiris, 2010; Blanke et al., 2015 for reviews). Especially the left parietal cortex has been involved in the visual coding of bodies of other people compared to one's own body (Felician et al., 2003, 2009; Corradi-Dell'acqua et al., 2008; Corradi-Dell'Acqua et al., 2009; Cleret de Langavant et al., 2012). Additionally, the cortical-subcortical network (parietal, basal ganglia and insular areas) involved in the present cardio-visual bodily effect has been linked to the sense of body ownership, both in body illusion paradigms using multisensory stimulation (Ehrsson et al., 2004; Lloyd et al., 2006; Tsakiris et al., 2007; Petkova et al., 2011) and by deficits of body ownership in neuropsychological studies (Cereda et al., 2002; Committeri et al., 2007; Gandola et al., 2012). Finally, our source localisation also indicates the role of left temporo-occipital regions, over and around the anterior part of EBA. It is well known that this brain region responds strongly to the vision of the human body and body parts (Downing et al., 2001; Peelen and Downing, 2007; Orlov et al., 2010; Bracci and Peelen, 2013; Harry et al., 2016). EEG studies also revealed that this region is the internal source of the N190 component, specific for body processing with respect to other categories of stimuli (Thierry et al., 2006).

In conclusion, the present study extends knowledge about the influence of cardiac information on visual perception and provides electrophysiological evidence for two major processing steps in visual information processing when analysing human visual bodies linked or not to the cardiac cycle. The first effect reflects a general enhancement of visual processing during cardiac synchronous stimulation, which is stimulus-independent and modulates the processing of both the early categorization of images and the later more complex visual analysis of bodily features. The second effect was focused on one category of stimuli, showing cardio-visual synchronous enhancement only for intact human body pictures but not scrambled bodies, partially overlapping with the time-window of the late stimulus-independent effect. This effect involves brain regions that have been shown to process the configuration or identity of the visually presented human body. The present data show that this mechanism is also modulated by cardiac interoceptive signals. A limitation of the present study is that we did not compare this latter effect with brain activity elicited by other bodily control stimuli (such as complete control objects or inverted bodies). Therefore, even if the comparison Body-intact vs. Body-scrambled revealed a differential brain activity (whole body vs. scrambled body), these results do not allow us to make any claims regarding the body-specificity of these cardiac effects.

There is now a growing interest in the role of interoceptive information in visual processing, and how this contributes to build the link between body, self, and consciousness (Craig, 2002; Seth, 2013). Even if previous evidence is on record about the mechanisms of cardio-visual integration, no study has shown the neural mechanisms and relevance for visual body processing. The present results establish the basis for future investigations about the neural correlates of bodily self-consciousness, and alteration of the bodily self through multisensory interoceptive-exteroceptive stimulation in healthy people and patients with disabling body representation disorders, as recently manipulated by cardio-visual stimulations (Aspell et al., 2013; Suzuki et al., 2013; Ronchi et al., 2015).

Acknowledgments

This work was supported by the Bertarelli Foundation and the Swiss National Science Foundation [grant number 320030_166643] to Olaf Blanke, and by the EPFL international fellowship program co-founded by the European Union's Seventh Framework Programme [grant number 291771] to Roberta Ronchi. The authors would like to thank Hyeong-Dong Park for his useful comments on a previous version of the manuscript.

References

Andersen, R.A., Snyder, L.H., Bradley, D.C., Xing, J., 1997. Multimodal representation of space in the posterior parietal cortex and its use in planning movements. Annu. Rev. Neurosci. 20, 303–330.

Ary, J.P., Klein, S.A., Fender, D.H., 1981. Location of sources of evoked scalp potentials: corrections for skull and scalp thicknesses. IEEE Trans. Biomed. Eng. 28, 447–452.

Aspell, J.E., Heydrich, L., Marillier, G., Lavanchy, T., Herbelin, B., Blanke, O., 2013. Turning body and self inside out: visualized heartbeats alter bodily self-consciousness and tactile perception. Psychol. Sci. 24, 2445–2453.

Barraclough, N.E., Xiao, D., Oram, M.W., Perrett, D.I., 2006. The sensitivity of primate STS neurons to walking sequences and to the degree of articulation in static images. Prog. Brain Res. 154, 135–148.

Beer, A.L., Plank, T., Meyer, G., Greenlee, M.W., 2013. Combined diffusion-weighted and functional magnetic resonance imaging reveals a temporal-occipital network involved in auditory-visual object processing. Front. Integr. Neurosci. 7, 5.

Bernasconi, F., Schmidt, A., Pokorny, T., Kometer, M., Seifritz, E., Vollenweider, F.X., 2014. Spatiotemporal brain dynamics of emotional face processing modulations induced by the serotonin 1A/2A receptor agonist psilocybin. Cereb. Cortex 24, 3221–3231.

Blanke, O., 2012. Multisensory brain mechanisms of bodily self-consciousness. Nat. Rev. Neurosci. 13, 556–571.

Blanke, O., 2014. Bodily sefl-consciousness. In: Gazzaniga, M., Mangun, G. (Eds.), The Cognitive Neurosciences. MIT Press, Cambridge, MA.

Blanke, O., Slater, M., Serino, A., 2015. Behavioral, neural, and computational principles of bodily self-consciousness. Neuron 88, 145–166.

Bracci, S., Peelen, M.V., 2013. Body and object effectors: the organization of object representations in high-level visual cortex reflects body–object interactions. J. Neurosci. 33, 18247–18258.

Brandman, T., Yovel, G., 2016. Bodies are represented as wholes rather than their sum of parts in the occipital-temporal cortex. Cereb. Cortex N. Y. N. 1991 26, 530–543.

Bremmer, F., Schlack, A., Duhamel, J.R., Graf, W., Fink, G.R., 2001. Space coding in primate posterior parietal cortex. NeuroImage 14, S46–S51.

Brozzoli, C., Makin, T.R., Cardinali, L., Holmes, N.P., Farnè, A., 2012. Peripersonal space: a multisensory interface for body–object interactions. In: Murray, M.M., Wallace, M.T. (Eds.), The Neural Bases of Multisensory Processes, Frontiers in Neuroscience. CRC Press/Taylor & Francis, Boca Raton (FL). Available at: http://www.ncbi.nlm.nih.gov/books/NBK92879/ (Accessed 2 June 2016).

Brunet, D., Murray, M.M., Michel, C.M., 2011. Spatiotemporal analysis of multichannel EEG: CARTOOL. Comput. Intell. Neurosci. 2011, 813870.

Bushara, K.O., Weeks, R.A., Ishii, K., Catalan, M.J., Tian, B., Rauschecker, J.P., Hallett, M., 1999. Modality-specific frontal and parietal areas for auditory and visual spatial localization in humans. Nat. Neurosci. 2, 759–766.

Calvert, G.A., 2001. Crossmodal processing in the human brain: insights from functional neuroimaging studies. Cereb. Cortex N. Y. N. 1991 11, 1110–1123.

Calvert, G.A., Campbell, R., Brammer, M.J., 2000. Evidence from functional magnetic resonance imaging of crossmodal binding in the human heteromodal cortex. Curr. Biol. CB 10, 649–657.

Cappe, C., Thelen, A., Romei, V., Thut, G., Murray, M.M., 2012. Looming signals reveal synergistic principles of multisensory integration. J. Neurosci. Off. J. Soc. Neurosci. 32, 1171–1182.

Cappe, C., Thut, G., Romei, V., Murray, M.M., 2010. Auditory–visual multisensory interactions in humans: timing, topography, directionality, and sources. J. Neurosci. 30, 12572–12580.

Cereda, C., Ghika, J., Maeder, P., Bogousslavsky, J., 2002. Strokes restricted to the insular cortex. Neurology 59, 1950–1955.
Chaumon, M., Bishop, D.V.M., Busch, N.A., 2015. A practical guide to the selection of independent components of the electroencephalogram for artifact correction. J. Neurosci. Methods 250, 47–63.
Cohen, Y.E., Andersen, R.A., 2004. Multimodal spatial representations in the primate parietal lobe. In: Spence, C., Driver, J. (Eds.), Crossmodal Space and Crossmodal Attention. Oxford, New York, pp. 99–121.
Cleret de Langavant, L., Trinkler, I., Remy, P., Thirioux, B., McIntyre, J., Berthoz, A., Dupoux, E., Bachoud-Lévi, A.-C., 2012. Viewing another person's body as a target object: a behavioural and PET study of pointing. Neuropsychologia 50, 1801–1813.
Committeri, G., Pitzalis, S., Galati, G., Patria, F., Pelle, G., Sabatini, U., Castriota-Scanderbeg, A., Piccardi, L., Guariglia, C., Pizzamiglio, L., 2007. Neural bases of personal and extrapersonal neglect in humans. Brain 130, 431–441.
Corradi-Dell'Acqua, C., Tomasino, B., Fink, G.R., 2009. What is the position of an arm relative to the body? Neural correlates of body schema and body structural description. J. Neurosci. Off. J. Soc. Neurosci. 29, 4162–4171.
Corradi-Dell'acqua, C., Ueno, K., Ogawa, A., Cheng, K., Rumiati, R.I., Iriki, A., 2008. Effects of shifting perspective of the self: an fMRI study. NeuroImage 40, 1902–1911.
Craig, A.D., 2002. How do you feel? Interoception: the sense of the physiological condition of the body. Nat. Rev. Neurosci. 3, 655–666.
Critchley, H.D., Wiens, S., Rotshtein, P., Ohman, A., Dolan, R.J., 2004. Neural systems supporting interoceptive awareness. Nat. Neurosci. 7, 189–195.
Daprati, E., Sirigu, A., Nico, D., 2010. Body and movement: consciousness in the parietal lobes. Neuropsychologia 48, 756–762.
de Gelder, B., Van den Stock, J., Meeren, H.K.M., Sinke, C.B.A., Kret, M.E., Tamietto, M., 2010. Standing up for the body. Recent progress in uncovering the networks involved in the perception of bodies and bodily expressions. Neurosci. Biobehav Rev. 34, 513–527.
Downing, P.E., Jiang, Y., Shuman, M., Kanwisher, N., 2001. A cortical area selective for visual processing of the human body. Science 293, 2470–2473.
Downing, P.E., Peelen, M.V., 2011. How might occipitotemporal body-selective regions interact with other brain areas to support person perception? Cogn. Neurosci. 2, 216–226.
Downing, P.E., Peelen, M.V., 2016. Body selectivity in occipitotemporal cortex: causal evidence. Neuropsychologia 83, 138–148.
Edwards, L., Inui, K., Ring, C., Wang, X., Kakigi, R., 2008. Pain-related evoked potentials are modulated across the cardiac cycle. Pain 137, 488–494.
Ehrsson, H.H., Spence, C., Passingham, R.E., 2004. That's my hand! Activity in premotor cortex reflects feeling of ownership of a limb. Science 305, 875–877.
Felician, O., Anton, J.-L., Nazarian, B., Roth, M., Roll, J.-P., Romaiguère, P., 2009. Where is your shoulder? Neural correlates of localizing others' body parts. Neuropsychologia 47, 1909–1916.
Felician, O., Ceccaldi, M., Didic, M., Thinus-Blanc, C., Poncet, M., 2003. Pointing to body parts: a double dissociation study. Neuropsychologia 41, 1307–1316.
Fort, A., Delpuech, C., Pernier, J., Giard, M.-H., 2002. Dynamics of cortico-subcortical cross-modal operations involved in audio-visual object detection in humans. Cereb. Cortex N. Y. N. 1991 12, 1031–1039.
Foxe, J.J., Schroeder, C.E., 2005. The case for feedforward multisensory convergence during early cortical processing. Neuroreport 16, 419–423.
Foxe, J.J., Wylie, G.R., Martinez, A., Schroeder, C.E., Javitt, D.C., Guilfoyle, D., Ritter, W., Murray, M.M., 2002. Auditory-somatosensory multisensory processing in auditory association cortex: an fMRI study. J. Neurophysiol. 88, 540–543.
Gandola, M., Invernizzi, P., Sedda, A., Ferrè, E.R., Sterzi, R., Sberna, M., Paulesu, E., Bottini, G., 2012. An anatomical account of somatoparaphrenia. Cortex 48, 1165–1178.
Garfinkel, S.N., Minati, L., Gray, M.A., Seth, A.K., Dolan, R.J., Critchley, H.D., 2014. Fear from the heart: sensitivity to fear stimuli depends on individual heartbeats. J. Neurosci. Off. J. Soc. Neurosci. 34, 6573–6582.
Gentile, G., Petkova, V.I., Ehrsson, H.H., 2011. Integration of visual and tactile signals from the hand in the human brain: an FMRI study. J. Neurophysiol. 105, 910–922.
Giard, M.H., Peronnet, F., 1999. Auditory-visual integration during multimodal object recognition in humans: a behavioral and electrophysiological study. J. Cogn. Neurosci. 11, 473–490.
Gliga, T., Dehaene-Lambertz, G., 2005. Structural encoding of body and face in human infants and adults. J. Cogn. Neurosci. 17, 1328–1340.
Grave de Peralta Menendez, R., Gonzalez Andino, S., Lantz, G., Michel, C.M., Landis, T., 2001. Noninvasive localization of electromagnetic epileptic activity. I. Method descriptions and simulations. Brain Topogr. 14, 131–137.
Grave de Peralta Menendez, R., Murray, M.M., Michel, C.M., Martuzzi, R., Gonzalez Andino, S.L., 2004. Electrical neuroimaging based on biophysical constraints. NeuroImage 21, 527–539.
Gray, M.A., Minati, L., Paoletti, G., Critchley, H.D., 2010. Baroreceptor activation attenuates attentional effects on pain-evoked potentials. Pain 151, 853–861.
Guthrie, D., Buchwald, J.S., 1991. Significance testing of difference potentials. Psychophysiology 28, 240–244.
Harry, B.B., Umla-Runge, K., Lawrence, A.D., Graham, K.S., Downing, P.E., 2016. Evidence for integrated visual face and body representations in the anterior temporal lobes. J. Cogn. Neurosci. 28, 1178–1193.
Ishizu, T., Amemiya, K., Yumoto, M., Kojima, S., 2010. Magnetoencephalographic study of the neural responses in body perception. Neurosci. Lett. 481, 36–40.
Khalsa, S.S., Rudrauf, D., Feinstein, J.S., Tranel, D., 2009. The pathways of interoceptive awareness. Nat. Neurosci. 12, 1494–1496.
Koenig, T., Kottlow, M., Stein, M., Melie-García, L., 2011. Ragu: a free tool for the analysis of EEG and MEG event-related scalp field data using global randomization statistics. Comput. Intell. Neurosci. 2011, 938925.
Koenig, T., Melie-García, L., 2010. A method to determine the presence of averaged event-related fields using randomization tests. Brain Topogr. 23, 233–242.
Koriath, J.J., Lindholm, E., 1986. Cardiac-related cortical inhibition during a fixed foreperiod reaction time task. Int. J. Psychophysiol. Off. J. Int. Organ Psychophysiol. 4, 183–195.
Lehmann, D., 1987. Handbook of electroencephalography and clinical neurophysiology. In: Gevins, A.S., Remond, A. (Eds.), Methods of Analysis of Brain Electrical Magnetic Signals, Principles of Spatial Analysis. Elsevier, Amsterdam, pp. 309–354.
Lehmann, D., Skrandies, W., 1980. Reference-free identification of components of checkerboard-evoked multichannel potential fields. Electroencephalogr. Clin. Neurophysiol. 48, 609–621.
Lewis, J.W., Van Essen, D.C., 2000. Corticocortical connections of visual, sensorimotor, and multimodal processing areas in the parietal lobe of the macaque monkey. J. Comp. Neurol. 428, 112–137.
Limanowski, J., Blankenburg, F., 2016. Integration of visual and proprioceptive limb position information in human posterior parietal, premotor, and extrastriate cortex. J. Neurosci. Off. J. Soc. Neurosci. 36, 2582–2589.
Lloyd, D., Morrison, I., Roberts, N., 2006. Role for human posterior parietal cortex in visual processing of aversive objects in peripersonal space. J. Neurophysiol. 95, 205–214.
Macaluso, E., Driver, J., 2001. Spatial attention and crossmodal interactions between vision and touch. Neuropsychologia 39, 1304–1316.
Martuzzi, R., Murray, M.M., Michel, C.M., Thiran, J.-P., Maeder, P.P., Clarke, S., Meuli, R.A., 2007. Multisensory interactions within human primary cortices revealed by BOLD dynamics. Cereb. Cortex N. Y. N. 1991 17, 1672–1679.
Mazzoni, P., Bracewell, R.M., Barash, S., Andersen, R.A., 1996. Spatially tuned auditory responses in area LIP of macaques performing delayed memory saccades to acoustic targets. J. Neurophysiol. 75, 1233–1241.
Michel, C.M., Murray, M.M., Lantz, G., Gonzalez, S., Spinelli, L., Grave de Peralta, R., 2004. EEG source imaging. Clin. Neurophysiol. Off. J. Int. Fed. Clin. Neurophysiol. 115, 2195–2222.
Molholm, S., Ritter, W., Murray, M.M., Javitt, D.C., Schroeder, C.E., Foxe, J.J., 2002. Multisensory auditory-visual interactions during early sensory processing in humans: a high-density electrical mapping study. Brain Res. Cogn. Brain Res. 14, 115–128.
Molholm, S., Sehatpour, P., Mehta, A.D., Shpaner, M., Gomez-Ramirez, M., Ortigue, S., Dyke, J.P., Schwartz, T.H., Foxe, J.J., 2006. Audio-visual multisensory integration in superior parietal lobule revealed by human intracranial recordings. J. Neurophysiol. 96, 721–729.
Montoya, P., Schandry, R., Müller, A., 1993. Heartbeat evoked potentials (HEP): topography and influence of cardiac awareness and focus of attention. Electroencephalogr. Clin. Neurophysiol. 88, 163–172.
Murray, M.M., Brunet, D., Michel, C.M., 2008. Topographic ERP analyses: a step-by-step tutorial review. Brain Topogr. 20, 249–264.
Orlov, T., Makin, T.R., Zohary, E., 2010. Topographic representation of the human body in the occipitotemporal cortex. Neuron 68, 586–600.
Park, H.-D., Bernasconi, F., Bello-Ruiz, J., Pfeiffer, C., Salomon, R., Blanke, O., 2016. Transient modulations of neural responses to heartbeats covary with bodily self-consciousness. J. Neurosci. Off. J. Soc. Neurosci. 36, 8453–8460.
Park, H.-D., Correia, S., Ducorps, A., Tallon-Baudry, C., 2014. Spontaneous fluctuations in neural responses to heartbeats predict visual detection. Nat. Neurosci. 17, 612–618.
Peelen, M.V., Downing, P.E., 2007. The neural basis of visual body perception. Nat. Rev. Neurosci. 8, 636–648.
Pekkola, J., Ojanen, V., Autti, T., Jääskeläinen, I.P., Möttönen, R., Sams, M., 2006. Attention to visual speech gestures enhances hemodynamic activity in the left planum temporale. Hum. Brain Mapp. 27, 471–477.
Perrin, F., Bertrand, O., Pernier, J., 1987. Scalp current density mapping: value and estimation from potential data. IEEE Trans. Biomed. Eng. 34, 283–288.
Petkova, V.I., Björnsdotter, M., Gentile, G., Jonsson, T., Li, T.-Q., Ehrsson, H.H., 2011. From part- to whole-body ownership in the multisensory brain. Curr. Biol. 21, 1118–1122.
Pourtois, G., Peelen, M.V., Spinelli, L., Seeck, M., Vuilleumier, P., 2007. Direct intracranial recording of body-selective responses in human extrastriate visual cortex. Neuropsychologia 45, 2621–2625.
Quinn, B.T., Carlson, C., Doyle, W., Cash, S.S., Devinsky, O., Spence, C., Halgren, E., Thesen, T., 2014. Intracranial cortical responses during visual-tactile integration in humans. J. Neurosci. Off. J. Soc. Neurosci. 34, 171–181.
Ronchi, R., Bello-Ruiz, J., Lukowska, M., Herbelin, B., Cabrilo, I., Schaller, K., Blanke, O., 2015. Right insular damage decreases heartbeat awareness and alters cardio-visual effects on bodily self-consciousness. Neuropsychologia 70, 11–20.
Salomon, R., Ronchi, R., Donz, J., Bello-Ruiz, J., Herbelin, B., Martet, R., Faivre, N., Schaller, K., Blanke, O., 2016. The insula mediates access to awareness of visual stimuli presented synchronously to the heartbeat. J. Neurosci. 36, 5115–5127.
Schlack, A., Sterbing-D'Angelo, S.J., Hartung, K., Hoffmann, K.P., Bremmer, F., 2005. Multisensory space representations in the macaque ventral intraparietal area. J. Neurosci. 25, 4616–4625.
Schandry, R., Montoya, P., 1996. Event-related brain potentials and the processing of cardiac activity. Biol. Psychol. 42, 75–85.
Schürmann, M., Kolev, V., Menzel, K., Yordanova, J., 2002. Spatial coincidence modulates interaction between visual and somatosensory evoked potentials. Neuroreport 13, 779–783.
Serino, A., Canzoneri, E., Avenanti, A., 2011. Fronto-parietal areas necessary for a multisensory representation of peripersonal space in humans: an rTMS study. J. Cogn. Neurosci. 23, 2956–2967.
Seth, A.K., 2013. Interoceptive inference, emotion, and the embodied self. Trends Cogn. Sci. 17, 565–573.

Soria Bauser, D.A., Suchan, B., 2013. Behavioral and electrophysiological correlates of intact and scrambled body perception. Clin. Neurophysiol. Off. J. Int. Fed. Clin. Neurophysiol. 124, 686–696.
Spinelli, L., Andino, S.G., Lantz, G., Seeck, M., Michel, C.M., 2000. Electromagnetic inverse solutions in anatomically constrained spherical head models. Brain Topogr. 13, 115–125.
Stein, B.E., Stanford, T.R., 2008. Multisensory integration: current issues from the perspective of the single neuron. Nat. Rev. Neurosci. 9, 255–266.
Suzuki, K., Garfinkel, S.N., Critchley, H.D., Seth, A.K., 2013. Multisensory integration across exteroceptive and interoceptive domains modulates self-experience in the rubber-hand illusion. Neuropsychologia 51, 2909–2917.
Talairach, J., Tournoux, P., 1988. Co-planar Stereotaxic Atlas of the Human Brain. Georg Thieme Verlag, Stuttgart. New York.
Teder-Sälejärvi, W.A., McDonald, J.J., Di Russo, F., Hillyard, S.A., 2002. An analysis of audio-visual crossmodal integration by means of event-related potential (ERP) recordings. Brain Res. Cogn. Brain Res. 14, 106–114.
Thelen, A., Cappe, C., Murray, M.M., 2012. Electrical neuroimaging of memory discrimination based on single-trial multisensory learning. NeuroImage 62, 1478–1488.
Thierry, G., Pegna, A.J., Dodds, C., Roberts, M., Basan, S., Downing, P., 2006. An event-related potential component sensitive to images of the human body. NeuroImage 32, 871–879.
Tsakiris, M., 2010. My body in the brain: a neurocognitive model of body-ownership. Neuropsychologia 48, 703–712.
Tsakiris, M., Hesse, M.D., Boy, C., Haggard, P., Fink, G.R., 2007. Neural signatures of body ownership: a sensory network for bodily self-consciousness. Cereb. Cortex 17, 2235–2244.
Urgesi, C., Berlucchi, G., Aglioti, S.M., 2004. Magnetic stimulation of extrastriate body area impairs visual processing of nonfacial body parts. Curr. Biol. CB 14, 2130–2134.
Vakli, P., Németh, K., Zimmer, M., Kovács, G., 2016. The electrophysiological correlates of integrated face and body-part perception. Q. J. Exp. Psychol. 2006, 1–12.
van Atteveldt, N., Murray, M.M., Thut, G., Schroeder, C.E., 2014. Multisensory integration: flexible use of general operations. Neuron 81, 1240–1253.
van Elk, M., Lenggenhager, B., Heydrich, L., Blanke, O., 2014. Suppression of the auditory N1-component for heartbeat-related sounds reflects interoceptive predictive coding. Biol. Psychol. 99, 172–182.
van Heijnsbergen, C.C.R.J., Meeren, H.K.M., Grèzes, J., de Gelder, B., 2007. Rapid detection of fear in body expressions, an ERP study. Brain Res. 1186, 233–241.
Walker, B.B., Sandman, C.A., 1982. Visual evoked potentials change as heart rate and carotid pressure change. Psychophysiology 19, 520–527.
Wiebking, C., Duncan, N.W., Tiret, B., Hayes, D.J., Marjańska, M., Doyon, J., Bajbouj, M., Northoff, G., 2014. GABA in the insula - a predictor of the neural response to interoceptive awareness. NeuroImage 86, 10–18.